

PAPER

Magnetic field profile of a mesoscopic SQUID-shaped superconducting film

To cite this article: F Rogeri *et al* 2013 *Supercond. Sci. Technol.* **26** 075005

View the [article online](#) for updates and enhancements.

Related content

- [Vortices in a mesoscopic superconducting disk of variable thickness](#)
E Sardella and E H Brandt
- [Vortices in superconductors: ideal lattice, pinning, and geometry effects](#)
Ernst Helmut Brandt
- [Nucleation of superconductivity and vortex matter in superconductor-ferromagnethybrids](#)
A Yu Aladyskhin, A V Silhanek, W Gillijns *et al.*

Recent citations

- [Frozen magnetic response in mesoscopic superconductors](#)
F Durán Flórez *et al*
- [Multi-vortex State Induced by Proximity Effects in a Small Superconducting Square](#)
J. Barba-Ortega *et al*



 **can
superconductors**

www.can-superconductors.com

HTS PARTS AND MATERIALS

Single and Multi-domain YBCO Bulk
REBCO Sputtering Targets
REBCO Powders and Granulates
BSCCO Current Leads, Magnetic Shields
Superconductivity Demonstration Kits

Magnetic field profile of a mesoscopic SQUID-shaped superconducting film

F Rogeri¹, R Zadorosny², P N Lisboa-Filho¹, E Sardella^{1,3} and W A Ortiz⁴

¹ UNESP-Universidade Estadual Paulista, Departamento de Física, Faculdade de Ciências, Caixa Postal 473, 17033-360, Bauru-SP, Brazil

² Departamento de Física e Química, Faculdade de Engenharia de Ilha Solteira, UNESP-Universidade Estadual Paulista, Caixa Postal 31, 15385-000 Ilha Solteira-SP, Brazil

³ UNESP-Universidade Estadual Paulista, IPMet-Instituto de Pesquisas Meteorológicas, CEP 17048-699 Bauru-SP, Brazil

⁴ Departamento de Física, Universidade Federal de São Carlos, 13565-905, São Carlos-SP, Brazil

E-mail: sardella@fc.unesp.br

Received 11 March 2013

Published 14 May 2013

Online at stacks.iop.org/SUST/26/075005

Abstract

Using a genuinely tridimensional approach to the time-dependent Ginzburg–Landau theory, we have studied the local magnetic field profile of a mesoscopic superconductor in the so-called SQUID geometry, i.e., a square with a hole at the center connected to the outside vacuum through a very thin slit. Our investigation was carried out in both the Meissner and the mixed state. We have also studied the influence of the temperature on the space distribution of the local magnetic field.

(Some figures may appear in colour only in the online journal)

1. Introduction

Demagnetizing effects, arising from the finiteness of real samples, become extremely important when the size of the specimen along the direction of the applied field is much smaller than the lateral dimensions of its cross section. In superconductors these effects—which are strongly dependent on the sample geometry—derive from the existence of a stray field produced by the shielding currents, which enhance the internal field near the edges of the sample. An important consequence is that, for superconducting films with thickness smaller than the temperature-dependent London penetration depth $\lambda(T)$, the decrease of fields and currents is not governed by $\lambda(T)$, as in bulk samples, but by an effective penetration depth which is inversely proportional to the thickness c of the sample, i.e., $\Lambda(T) = \lambda^2(T)/c$. With this effective length, in opposition to what occurs in bulk materials, a non-exponential long-range interaction of vortices takes place, since the currents interact with the stray fields generated by themselves. In this case, as was first reported by Pearl [1], vortex–vortex interactions decay as $1/r^2$, being thus much more repulsive than in the case of Abrikosov vortices. As a consequence,

the value of the local magnetic field at the surface, required to nucleate vortices and keep them inside the film, is larger than the equivalent for bulk samples, which is merely the applied field. This is intimately related to what is usually called demagnetization effects.

The study of these features in superconducting thin films are of particular importance for potential applications, such as, for example, in the fabrication of microwave circuits [2], in the development of atom chips [3], i.e., superconducting devices which trap cold atoms, and in the production of superconducting quantum interference devices (SQUIDs) [4]. In 2007, Brandt and Mikitik [5] studied what is known as the shaking effect, considering an inclined DC magnetic field and a small AC field (the shaking field) applied parallel to the plane of a superconducting thin film. Thus, using the Bean approach, they obtained an anisotropic relaxation of the internal field and sheet currents over the sample. Some studies by Brandt [6, 7], and by Clem and Brandt [8], described the distribution of the internal field and the sheet currents in thin films shaped in the so-called SQUID geometry, employing some variations for the cross section of the sample. The authors considered that finite films could be described by the

London theory, expressing the sheet currents and part of the coupling flux between the vortices and the holes or slits, by a stream function. London's and Maxwell's equations were averaged along the z direction. As a result, a 3D problem was mapped into a 2D solution of these equations with $\lambda(T)$ replaced by $\Lambda(T)$.

In the present work we carried out the study of a thin film in a SQUID geometry using the three-dimensional time-dependent Ginzburg–Landau (3D-TDGL) theory. To our knowledge, this is the first attempt to address such a relevant problem by employing a genuinely 3D approach. Our results confirm and extend those obtained on the illuminating work reported in [6–8], for which the London theory was applied.

This paper is organized as follows. In section 2 we present a brief summary of the TDGL equations and how we solve them. In section 3 we apply this formalism to a superconducting film in the SQUID geometry and show the corresponding magnetic field profiles. Also, we investigate the universality of these profiles with the parameter $\Lambda(T)$, as was left implicit in [6], as well as the influence of the temperature on the magnetic field distributions. In section 4 we present our conclusions.

2. Theoretical formalism

The TDGL formalism is a useful tool to describe a great variety of phenomena in superconductors. It is a set of two equations which couple the two fundamental quantities of the superconducting state, namely, the order parameter ψ and the vector potential \mathbf{A} . The superconducting electronic density of Cooper pairs is given by $|\psi|^2$ and the local magnetic field profile is obtained through $\mathbf{B} = \nabla \times \mathbf{A}$. According to [9] the non-dimensional version of these equations is given by

$$\begin{aligned} \left(\frac{\partial}{\partial t} + i\phi \right) \psi &= -(-i\nabla - \mathbf{A})^2 \psi + (1 - T)\psi(1 - |\psi|^2), \\ \beta \left(\frac{\partial \mathbf{A}}{\partial t} + \nabla \phi \right) &= \mathbf{J}_s - \kappa^2 \nabla \times \mathbf{B}, \end{aligned} \quad (1)$$

where the supercurrent density is

$$\mathbf{J}_s = (1 - T) \text{Re} [\bar{\psi} (-i\nabla - \mathbf{A}) \psi]. \quad (2)$$

The boundary conditions are

$$\begin{aligned} \hat{\mathbf{n}} \cdot (-i\nabla - \mathbf{A}) \psi &= 0, & \text{on } \partial\Omega, \\ \nabla \times \mathbf{A} &\rightarrow \mathbf{H}, & \text{as } |\mathbf{r}| \rightarrow \infty, \end{aligned} \quad (3)$$

where \mathbf{H} is the uniformly applied external magnetic field; Ω is the domain occupied by the superconducting material, and $\hat{\mathbf{n}}$ is an outward unit vector, normal to the superconductor–vacuum interface $\partial\Omega$.

The notation employed in the present work is such that the temperature, T , is expressed in units of the critical temperature, T_c ; the distances are measured in units of the zero-temperature coherence length, $\xi(0)$; the magnetic field is in units of the zero-temperature upper critical field, $H_{c2}(0)$; the time is in units of the characteristic time $t_0 = \pi\hbar/8K_B T_c$ [10]; $\kappa = \lambda(T)/\xi(T) = \lambda(0)/\xi(0)$ is the Ginzburg–Landau parameter; β is the relaxation time of the

vector potential; and the symbol Re denotes the real part of a complex function. Note that equations (1) and (2) are gauge invariant, since they do not change under the transformation $\psi' = \psi e^{i\chi}$, $\mathbf{A}' = \mathbf{A} + \nabla\chi$, $\phi' = \phi - \partial\chi/\partial t$. We choose the zero-scalar potential gauge, that is, $\phi' = 0$ at all times.

The TDGL equations have been very useful to simulate how vortices can be arranged as an external magnetic field (either abruptly or adiabatically increased) is applied to a superconductor below its critical temperature. Since equations (1) do not have exact solutions, many discretization algorithms have been devised for solving them numerically. One of the most popular approaches is the gauge-invariant link variables method (see for instance [11] for the solution of a 3D problem, and [12] for 2D problems). In [13], this method was generalized to circular geometries. It was also adapted and successfully employed to disks with a variable degree of roughness on the surface [14].

Usually, equations (1) are solved numerically in two different scenarios. One is that in which the system has invariance along the z direction if the external field is applied along the same direction; this is the case of a long cylinder, either of circular or rectangular cross section. Within this scenario, we have a true 2D problem for which the physical quantities vary only with the x and y coordinates and demagnetization effects are not present, that is, the local magnetic field outside the sample is the external applied magnetic field \mathbf{H} . The other typical scenario is when the system is a very thin film, for which the first TDGL equation for the order parameter is solved only at the xy plane and the second equation is solved by substituting the supercurrent density with a superconducting sheet current density

$$\mathbf{J}_s = c\delta(z)(1 - T) \text{Re} [\bar{\psi} (-i\nabla - \mathbf{A}) \psi], \quad (4)$$

where c is the thickness of the superconducting film. This replacement is equivalent to an average process of the TDGL equations along the z direction, being a simplification valid only if $c \ll \lambda(T)$ [1]. Although in this case the solution of the TDGL equations is significantly simplified, the demagnetization effects are not neglected.

Both limits of the TDGL equations are very useful to extract the most relevant physical properties of mesoscopic superconductors. However, in one situation we lose important information concerning the demagnetization effects which are always present, whereas, for the other, the results will be limited to very thin films. In the present work we solve the true 3D-TDGL equations for a SQUID as sketched in figure 1 by using the algorithm developed in [11]. The SQUID has width a , length b , and thickness c . The size of the hole is indicated by h_x and h_y and the direction of the slit coincides with the x axis. The system is considered inside a simulation box of dimensions $\mathcal{A} \times \mathcal{B} \times \mathcal{C}$ (not shown in figure 1). The size of the simulation box is taken sufficiently large to ensure that the local magnetic field equals \mathbf{H} at its faces⁵.

⁵ The faces which we are referring to are the $x = \pm\mathcal{A}/2$, $y = \pm\mathcal{B}/2$, $z = \pm\mathcal{C}/2$ planes.

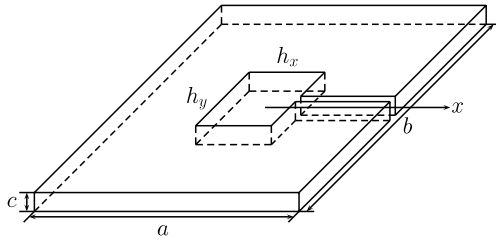


Figure 1. Schematic view of a mesoscopic superconducting SQUID. The external applied magnetic field H is perpendicular to the plane of the SQUID.

3. Results and discussion

The SQUID of figure 1 has been studied in [6] by using the London equation and the Biot–Savart law to determine the local magnetic field both inside and outside the superconductor. The results of this approach suggest that the local magnetic field along the slit of the SQUID (in units of the applied field) $B_z(x, 0, 0)/H$ obeys a scaling law which depends exclusively on the effective penetration length $2\Lambda(T)/a = 2\lambda^2(T)/ac$ (in units of $a/2$), regardless of the individual values of $\lambda(T)$, a and c . In our units, and assuming that $\lambda(T) = \lambda(0)/\sqrt{1-T}$, this corresponds to $2\Lambda(T)/a = 2\kappa^2/ac(1-T)$, where on the right-hand side of the last relation a and c are in dimensionless units.

Since within the London model the order parameter is assumed to be constant everywhere, one can reasonably expect that results arising from such a treatment will be less accurate than those obtained from a more comprehensive theory, such as the one employed here. To allow a direct comparison of our results with those of [6, 7], one has to consider that Brandt did not introduce the explicit temperature dependence of $\lambda(T)$, which can be mimicked by choosing $T = 0$, in which case the TDGL equations have the same form as those obtained using $\xi(T)$ as the unit length. For this reason, the results presented in figures 2–6 refer to $T = 0$. The presentation and discussions of the temperature dependence of our results is postponed to the final part of the manuscript. Another important observation is that all values of κ indicated in the figures throughout the paper were taken with a sufficient number of decimal places in order to make the value of $2\Lambda(0)/a$ exact.

In figure 2 we have plotted the local field along the x axis, which passes through the slit and the hole of the SQUID (as shown in figure 1), for several values of H . The dimensions of the superconductor are taken as $12 \times 12 \times 1$, the simulation box as $19 \times 19 \times 11$, and the hole as 2.4×2.4 .⁶ We used the resolution of the mesh as ten points per $\xi(0)$ in all directions. As can be seen from this figure, the profile of the magnetic field $B_z(x, 0, 0)/H$ is very weakly dependent on H within the Meissner state (curves with $H = 0.1$ and 0.3). Note that the spatial distribution of $B_z(x, 0, 0)/H$ is very similar to that found in [6, 7], namely, a maximum within the slit, and a

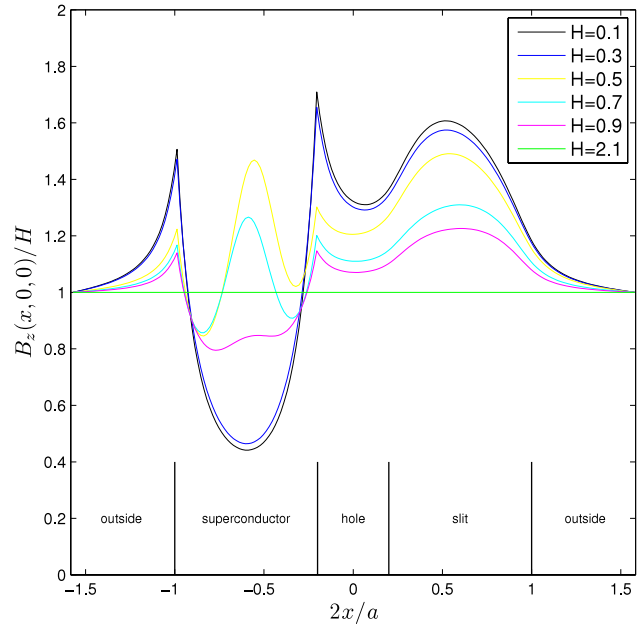


Figure 2. Intensity of the z component of the local magnetic field, normalized to the external applied field, along the x axis for several values of H . SQUID dimensions are $12 \times 12 \times 1$ and the Ginzburg–Landau parameter is $\kappa = 0.774\,596\,669$.

minimum inside the hole. As the mixed state sets in (i.e., for curves with $H \geq 0.5$ in figure 2), the profile of the magnetic field inside the superconductor changes significantly, as one should expect, due to the presence of vortices (which can be seen in figure 3). On the other hand, along the slit and the hole, the magnetic field tends to diminish with increasing applied fields, although the overall behavior of the curve remains unchanged. The reason for such a tendency is that an extra magnetic field outside the superconductor is generated by the supercurrents, which enhances the local field. However, as vortices nucleate inside the superconductor, the shielding supercurrent density is weakened, and so is the stray field. Another interesting characteristic of the $B_z(x, 0, 0)/H$ curve is that, at the slit, the field is enhanced to as much as $1.6H$, whereas from [6, 7] the prediction for $2\Lambda(0)/a = 0.1$ is $\sim 2.6H$. It becomes clear that the London theory overestimates the enhanced field along the slit and the hole. Still concerning figure 2, we can see that in the Meissner state, the local magnetic field penetrates over a distance which is larger than $\lambda(0)$ (κ in our units). This also occurs in the cases discussed in [6–8] because, for a film, the penetration of the field is controlled solely by $2\Lambda(T)/a$ and not κ , as is the situation when we do not have demagnetization effects.

The upper panel of figure 3 is an intensity plot of the local magnetic field in the $z = 0$ plane. The intensity of the field is shown in the color bar. For $H = 0.3$ the superconductor is still in the Meissner state, whereas for $H \geq 0.5$ it is already in the mixed state. As H increases, vortices penetrate through the left side of the SQUID, but not along the slit. This is due to the fact that the shielding currents on the outer face opposite the slit are smaller than along the other faces of the SQUID, so that the field is largely enhanced in the slit. Initially, once the vortices start nucleating inside the sample, some of them will

⁶ In all the cases we have considered $a = b$. Furthermore, in order to make a comparison of our results with those of [6] on an equal footing, we have taken the size of the hole such that its dimension corresponds to $h_x = h_y = 0.2a$.

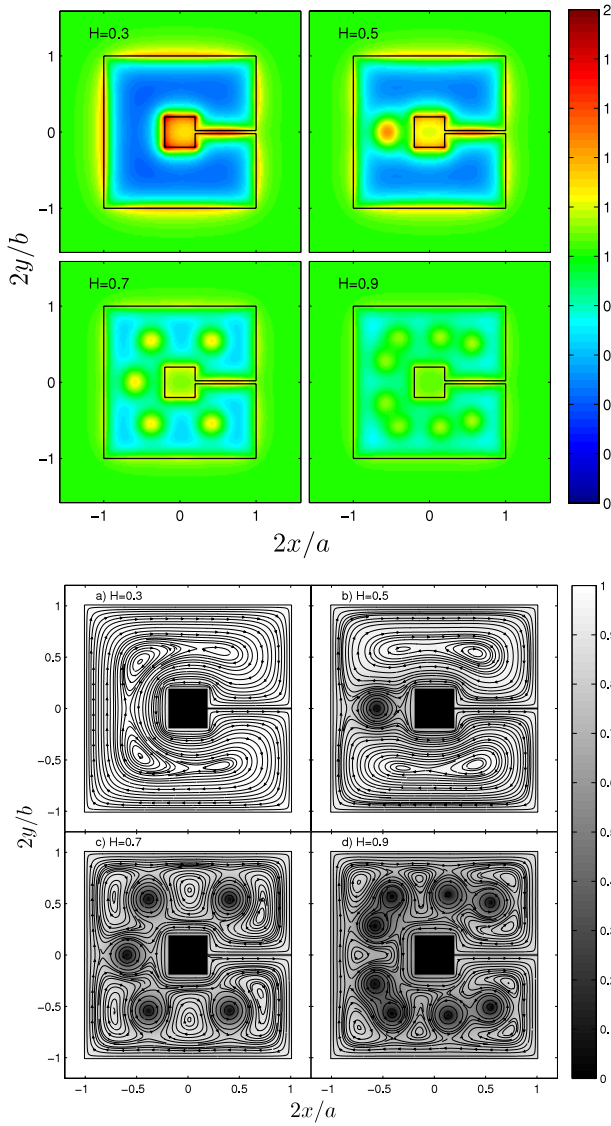


Figure 3. (Upper panel) Intensity plot of the z component of the local magnetic field, $B_z(x, 0, 0)/H$, at the $z = 0$ plane for several values of H : for $H = 0.3$ the SQUID is still in the Meissner state; for $H \geq 0.5$ the mixed state is already nucleated with $N = 1$ vortex in the superconductor and 2 in the hole for $H = 0.5$, $N = 5$ vortices in the superconductor and 2 in the hole for $H = 0.7$, and $N = 8$ vortices in the superconductor and 3 in the hole for $H = 0.9$. (Lower panel) The intensity of the order parameter with current density streamlines superimposed.

be captured by the hole and some others will be distributed around it. Note that when the number of vortices in the hole saturates, they stay as far as possible from the slit, where the shielding currents are larger. In the lower panel of figure 3 we show the intensity of the order parameter with current density streamlines superimposed.

According to [6, 7], the field at the slit and the hole is further enhanced as $2\Lambda(T)/a$ decreases. We have tested this tendency by changing a while both κ and c were kept fix. Figure 4 shows two curves of $B_z(x, 0, 0)/H$ for two distinct values of a . Indeed, as $2\Lambda(T)/a$ decreases, the field becomes larger everywhere outside the sample, and the magnetic response is even more diamagnetic along the superconducting

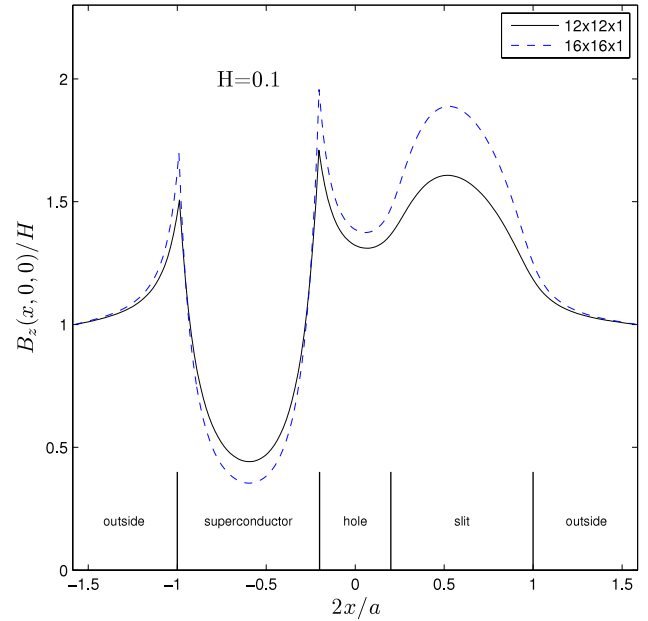


Figure 4. The same as in figure 2 for two SQUIDs of distinct widths and lengths, the same thickness, and the same Ginzburg–Landau parameter $\kappa = 0.774\,596\,669$. The parameters were chosen such that for the smaller SQUID $2\Lambda(0)/a = 0.1$ and for the larger one $2\Lambda(0)/a = 0.075$.

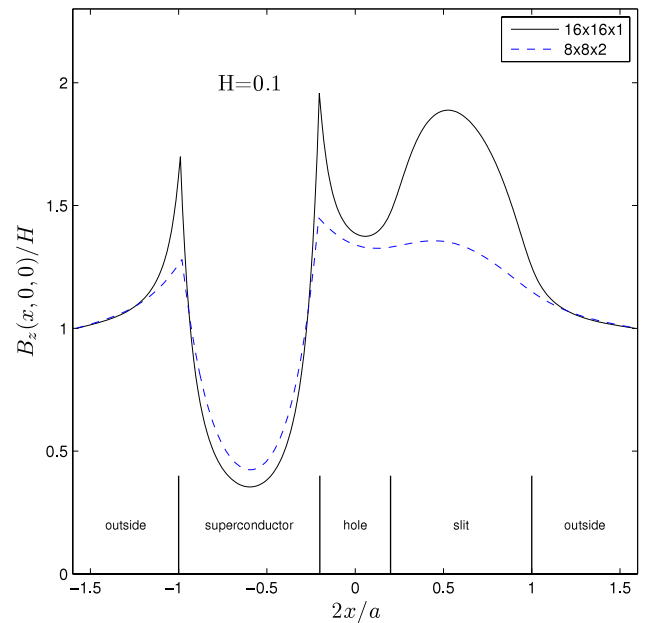


Figure 5. The same as in figure 2 for two SQUIDs of distinct dimensions and the same Ginzburg–Landau parameter $\kappa = 0.774\,596\,669$. The parameters were chosen such that for both SQUIDs we have the same $2\Lambda(0)/a = 0.075$.

core. Quantitatively, however, the enhancement is not as large as predicted by London theory.

We have gone further on investigating the independence of $B_z(x, 0, 0)/H$ with respect to the parameters κ , a and c , although not individually but rather through $2\Lambda(T)/a = 2\lambda^2(T)/ac$. In fact, in the London approach for a very thin film one can average both the 3D London and Maxwell equations

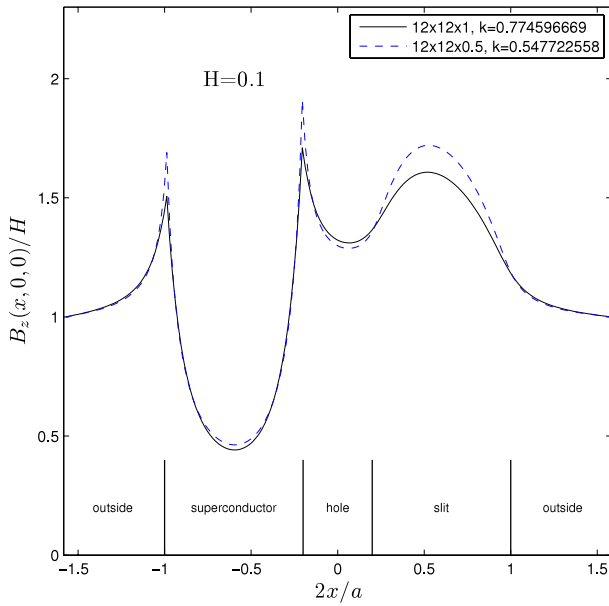


Figure 6. The same as in figure 2 for two SQUIDs of the same width and length and distinct thickness. Both SQUIDs have different Ginzburg–Landau parameters. Although characterized by different parameters, both SQUIDs have $2\Lambda(0)/a = 0.1$.

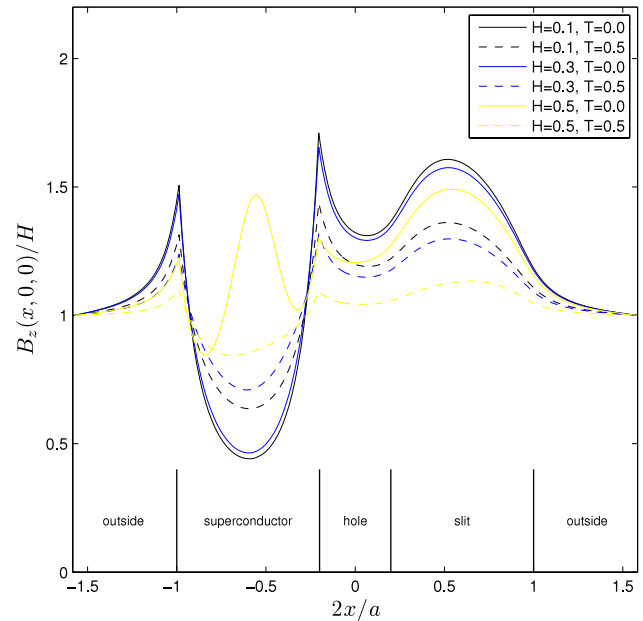


Figure 7. The same as in figure 2 for a SQUID of dimensions $12 \times 12 \times 1$ at two different temperatures.

along the z direction, and map a 3D problem into a 2D one, although the true three-dimensional nature of the original problem is not lost after carrying out this simplification. In this manner, the equations have a single parameter, namely, $\Lambda(T)$. Nevertheless, in the 3D Ginzburg–Landau approach we always have a dependence on the material through the parameter κ and the dimensions of the superconductor. In this part of the investigation the goal was to verify whether the full Ginzburg–Landau equations, without any simplification, exhibit the same scaling law.

In figure 5 we depict two $B_z(x, 0, 0)/H$ curves for two SQUIDs with different dimensions, a and c , but with the same value of κ . In both cases, $2\Lambda(0)/a = 0.075$. As can be seen in the figure, from one curve to the other the field profile varies throughout the whole SQUID, including the superconductor core as well as the slit and the hole, and the universal behavior predicted by London theory does not hold in the 3D Ginzburg–Landau approach. Finally, in figure 6, we show the same curves for different values of c and κ , but keeping the lateral dimensions of the film a fixed. As can be seen from this figure, the local field exhibits different profiles both inside and outside the SQUIDs, although not as much as in the previous case.

We have also investigated the influence of the temperature on the local magnetic field distribution of the SQUID. In figure 7 we have plotted the field profile for two values of the temperature. One can clearly see that, as the applied magnetic field increases, the enhancement of the local field becomes much less important for larger temperatures. This is consistent with the fact that the higher the temperature, the more uniform the local field inside the superconductor should be, and the weaker the superconducting sheet current density. As a consequence, the interaction of the currents with the stray fields are weakened as T increases.

4. Conclusions

Using the 3D-TDGL approach we have studied the local field distribution associated with a thin superconducting film in the so-called SQUID geometry. To our knowledge, this is the first report of a genuinely 3D solution for this problem. Previous results, obtained by Brandt and Clem [6–8] in the framework of the London theory, were revisited and compared to those obtained here. As expected, although the general trends are quite similar, the agreement is usually of a qualitative nature. In particular, we have shown that the universality of the field profiles with respect to the parameter $2\Lambda(T)/a$, implied by the treatment within the London theory, does not hold when the 3D-TDGL approach is employed. This limitation is not surprising, since the London approach should be recovered from our 3D-TDGL treatment only in the limit of extremely large κ .

Acknowledgments

The authors thank the Brazilian Agencies FAPESP and CNPq for financial help.

References

- [1] Pearl J 1964 *Appl. Phys. Lett.* **5** 65
- [2] Klein N 2002 *Rep. Prog. Phys.* **65** 1387
- [3] Sokolovsky V, Prigozhin L and Dikovskiy V 2010 *Supercond. Sci. Technol.* **23** 065003 (and references 2 to 9 of this paper)
- [4] ter Brake H J M 2006 *Physica C* **439** 1
- [5] Brandt E H and Mikitik G P 2007 *Supercond. Sci. Technol.* **20** S111 and references therein
- [6] Brandt E H 2005 *Phys. Rev. B* **72** 024529
- [7] Brandt E H 2005 *Physica C* **460** 327

- [8] Clem J R and Brandt E H 2005 *Phys. Rev. B* **72** 174511
- [9] Schmid A 1966 *Phys. Kondens. Mater.* **5** 302
- [10] Werthamer N R 1969 *Superconductivity* ed R D Parks (New York: Dekker)
- [11] Groop W D, Kaper H G, Leaf G K, Levine D M, Palumbo M and Vinokur V M 1996 *J. Comput. Phys.* **123** 254
- [12] Buscaglia G C, Bolech C and López A 2000 *Connectivity and Superconductivity* ed J Berger and J Rubinstein (Heidelberg: Springer)
- [13] Sardella E, Lisboa-Filho P N and Malvezzi A L 2008 *Phys. Rev. B* **77** 104508
- [14] Sardella E and Brandt E H 2011 *Supercond. Sci. Technol.* **23** 025015